

## Creep Motion of an Intruder within a Granular Glass Close to Jamming

R. Candelier and O. Dauchot

*SPEC, CEA-Saclay, URA 2464 CNRS, 91 191 Gif-sur-Yvette, France*  
(Received 15 June 2009; published 17 September 2009)

We experimentally study the dynamics of an intruder dragged at a constant force in a horizontally vibrated monolayer of grains. At moderate packing fractions, the intruder moves rapidly as soon as the force is applied. Above some threshold value it has an intermittent creep motion with strong fluctuations reminiscent of “crackling noise”. These fluctuations are critical at the jamming transition  $\phi_J$  unveiled in a previous study. The transition separates a regime with local free volume rearrangements from a regime where the displacement field is strongly heterogeneous and resembles force chain patterns.

DOI: 10.1103/PhysRevLett.103.128001

PACS numbers: 45.70.-n, 83.80.Fg

The understanding of the mechanical properties of amorphous media such as granular media, foams, emulsions, suspensions or structural glasses has raised formidable interest in the past decades [1]. At high packing fractions, such materials eventually jam and sustain a finite shear stress before yielding [2–4]. Several experiments on granular systems have emphasized the role of dynamical heterogeneities in the glassy like increase of the structural relaxation time [5]. More recently it was shown that dynamical heterogeneities, albeit of another type, also control the time scales of the jamming transition of a horizontally vibrated granular monolayer [6]. However these experiments do not provide any direct measurement of a mechanical response function. Conversely many experiments report on the stress-strain relation in dense granular packings [7], but do not have an easy access to the dynamics of individual grains. Investigating the drag of an intruder, the subject of this Letter, is a possible way of bridging the gap between dynamical and mechanical properties. Experiments in colloids [3], foams [2] and granular media [8–11] as well as simulations of structural glasses [12] were performed along this line. For loose packings and large drag, that is in the so-called fluidized regime, the velocity dependence of the drag force  $F$  follows Stokes’ law,  $F \propto V$  [8]. For denser packings, experiments report either  $F \simeq \text{cst}$  or  $F \propto \ln(V)$  [2,9–11] when the velocity is fixed, and  $F = F_Y + V^\gamma$ , with  $\gamma \leq 1$  and  $F_Y$  a finite yield force, when the force is imposed [3,12]. In both cases, the dynamics has been described as very intermittent. Stress fluctuations have been investigated in detail in [10], but very little is known about the displacement field and the velocity fluctuations.

In this Letter we study the dynamics of an intruder dragged by a constant force, in a bidisperse monolayer of horizontally vibrated grains. The experiment is run in the same setup (Fig. 1) and following the same protocol as in [6], where the jamming transition has been identified without ambiguity: at  $\phi_J$  the pressure measured in the absence of vibration vanishes and dynamical heterogeneities exhibit a critical behavior. Here, we observe that close to  $\phi_J$ ,

the intruder motion is reminiscent of a “crackling noise” signal [13], with critical fluctuations at the transition. Investigating the displacements and the free volume fields around the intruder, we conclude that the transition separates a regime dominated by local free volume rearrangements from a regime dominated by the rearrangements of the force network. This transition is distinct from fluidization [11], observed at a looser packing fraction which depends on the applied force, when the intruder recovers a continuous motion.

The experimental setup (Fig. 1) has been described elsewhere and we shall only recall here its most important elements together with the modifications imposed by the drag of the intruder. A monolayer of 8500 bidisperse brass cylinders of diameters  $d_{\text{small}} = 4/5 d_{\text{big}} = 4 \pm 0.01$  mm lays out on a horizontal glass plate vibrated horizontally ( $f = 10$  Hz,  $A = 10$  mm). The grains are confined in a cell fixed in the laboratory frame. The packing fraction,  $\phi$ , can be varied by tiny amounts ( $\delta\phi/\phi \sim 5 \times 10^{-4}$ ) and the pressure exerted on the moving lateral wall is measured by a force sensor. The intruder consists in a larger particle of same height ( $d_{\text{intruder}} = 2 \cdot d_{\text{small}}$ ) introduced in the system and pulled by a mass  $M$  via a pulley perpendicularly to the vibration. The fishing wire, which stands over the other

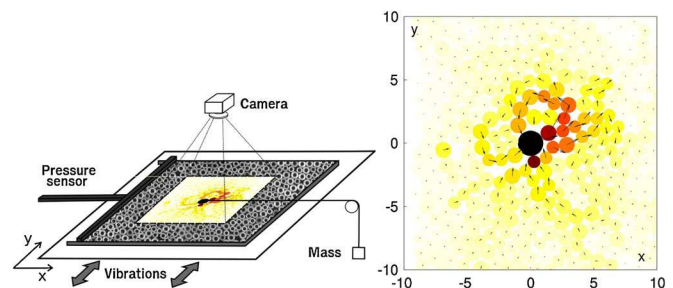


FIG. 1 (color online). *Left*: a monolayer of disks is vibrated horizontally, while dragging an intruder at constant force. Both the intruders and the surrounding grains are tracked by a CCD camera; *Right*: a strongly intermittent and heterogeneous response is observed, see text for details.

grains, does not disturb the dynamics. Most of the results presented here are related to experiments performed at a constant force ( $F_1 = 0.67N$ ,  $F_2 = 1.48N$ ,  $F_3 = 2.62N$ ) and varying the packing fraction  $\phi$  in the range  $[0.82-0.85]$  but we also conducted experiments at constant packing fractions, ( $\phi_1 = 0.8383$ ,  $\phi_2 = 0.8394$ ,  $\phi_3 = 0.8399$ ) increasing the force from  $0.67N$  to  $14.25N$ . For comparison, the total weight of the grains is  $23.11N$  and the force registered at the wall when the grains are highly compressed is of the order of  $50N$ . Note that in the present study the inertial time scale  $t_{in} = \sqrt{md/F} = 10^{-3}$  is always much shorter than the vibration one. Also the typical acceleration of the intruder never exceeds  $0.2 \text{ ms}^{-2}$  so that  $m \frac{d^2x}{dt^2}$  is always much smaller than  $F = Mg$ . The motion is completely overdamped and the elementary time scale is really that of the vibration. The time unit is set to one plate oscillation while the length unit is chosen to be the diameter of the small particles.

Starting from a low packing fraction  $\phi$ , we gradually compress the system until it reaches a highly jammed state following the same protocol as in [6]. Then we stepwise decrease the volume fraction. In the absence of an intruder, it was shown that the average relaxation time increases monotonically with the packing fraction, while the dynamics exhibits strong dynamical heterogeneities, the length scale and time scale of which exhibit a sharp peak at an intermediate packing fraction. The pressure measured at the wall in the absence of vibration falls to zero precisely below that packing fraction, hence called the jamming transition  $\phi_J$ . In the present study, the intruder is inserted at its initial position in place of one big and two small grains before each downward step in the packing fraction and the system is kept under vibration until the pressure has recovered its value in the absence of the intruder. Only then the force is applied on the wire and the intruder is dragged through the cell, while its motion together with that of a set of 1800 surrounding grains is tracked by a digital video camera triggered in phase with the oscillations of the plate.

At low packing fraction, and large enough force, the intruder motion is continuous. When increasing the packing fraction, it becomes intermittent above some threshold, which increases with the applied force (Fig. 2, left). Performing experiments at a given packing fraction and increasing the force, one observes that the applied force is proportional to the average velocity of the intruder  $F \propto V$  in the continuous motion regime, whereas  $F \propto \ln V$  in the intermittent one (Fig. 2, right). We thereby identify this transition with the fluidization one [11]. Note that for the largest packing fraction  $\phi_2$  and  $\phi_3$ , we could not observe the fluidization. As a result, there is a very strong contrast between the continuous motion of the intruder observed at  $\phi = \phi_1$  for large enough forces, say  $F = 10N$ , and the strongly intermittent one observed at  $\phi = \phi_2$  for the same large force. Typically the intruder averaged velocity loses 3 orders of magnitude and its velocity fluctuations gain more

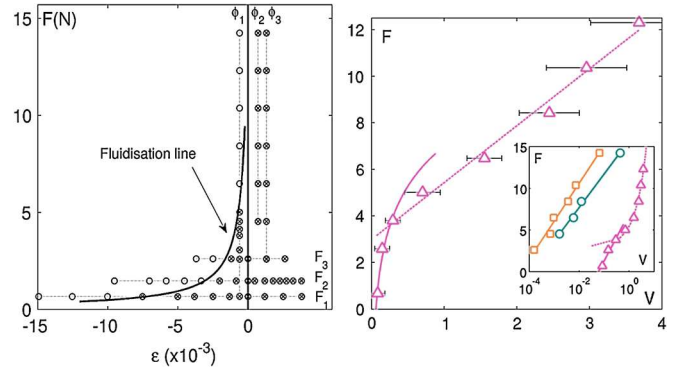


FIG. 2 (color online). From flow to jammed states: *Left*: Parameter space, (force  $F$ —relative packing fraction  $\epsilon = (\phi - \phi_J)/\phi_J$ ): at low  $\phi$  and large  $F$ , ( $\circ$ ) the packing is fluidized, the intruder motion is continuous and  $F \propto V$ ; at large  $\phi$  and low  $F$  ( $\otimes$ ), the intruder exhibits an intermittent motion and  $F \propto \ln V$ . The horizontal and vertical dotted lines indicate the path followed in the parameter space in the present study. *Right*:  $F$  versus  $V$  along the paths  $\phi_1$  ( $\Delta$ ),  $\phi_2$  ( $\circ$ ) and  $\phi_3$  ( $\square$ ); *Inset*: same in log-lin.

than 5 orders of magnitude, while  $\phi$  is increased by less than 1%, already suggesting the existence of a sharp transition.

We now focus on the experiments performed at constant and rather small force. When looking at the intruder displacements  $\delta x$  along the dragging direction during one vibration cycle (Fig. 3, top left), one immediately notices very strong fluctuations, with bursts of widely fluctuating magnitude. More quantitatively, the probability density functions of  $\delta x$  (Fig. 3, middle left) exhibit an important skewness towards the positive displacements. We characterize the positive part of the distribution, i.e., the displacements in the direction of the drag force,  $\delta x^+$ , by computing the average value  $\mu^+ = \langle \delta x^+ \rangle$  and the relative fluctuations  $\sigma^+/\mu^+ = \langle (\delta x^+ - \mu^+)^2 \rangle^{1/2}/\mu^+$ . One observes (Fig. 3, bottom left) that  $1/\mu^+$  increases continuously by 3 orders of magnitude, while varying the packing fraction of only a few percent,  $\delta\phi/\phi = 2 \times 10^{-2}$ , and that  $\sigma^+/\mu^+$  exhibits a peak at an intermediate packing fraction. Both behaviors are directly reminiscent of what has been recalled above for the dynamics in the absence of an intruder. We could check indeed that the peak observed in the fluctuations of the intruder motion coincides with a vanishing pressure in the absence of vibration and thereby locate it at  $\phi_J$  without ambiguity. Note however that the precise value of  $\phi_J$  depends on the precise packing that has been selected when the system has been compressed and that the small and nonmonotonic variations of  $\phi_J = 0.8369$ ,  $0.8383$ ,  $0.8379$  for the three forces  $F_1$ ,  $F_2$ ,  $F_3$  together with the small difference with the value  $\phi_J = 0.842$  reported in [6] must be attributed to differences in the initial conditions and more generally in the compression protocol (see [14,15] for a detailed discussion in the case of hard spheres). Figure 3, bottom left, displays both  $1/\mu^+$  and  $\sigma^+/\mu^+$  as a function of  $\epsilon = (\phi - \phi_J)/\phi$  the relative

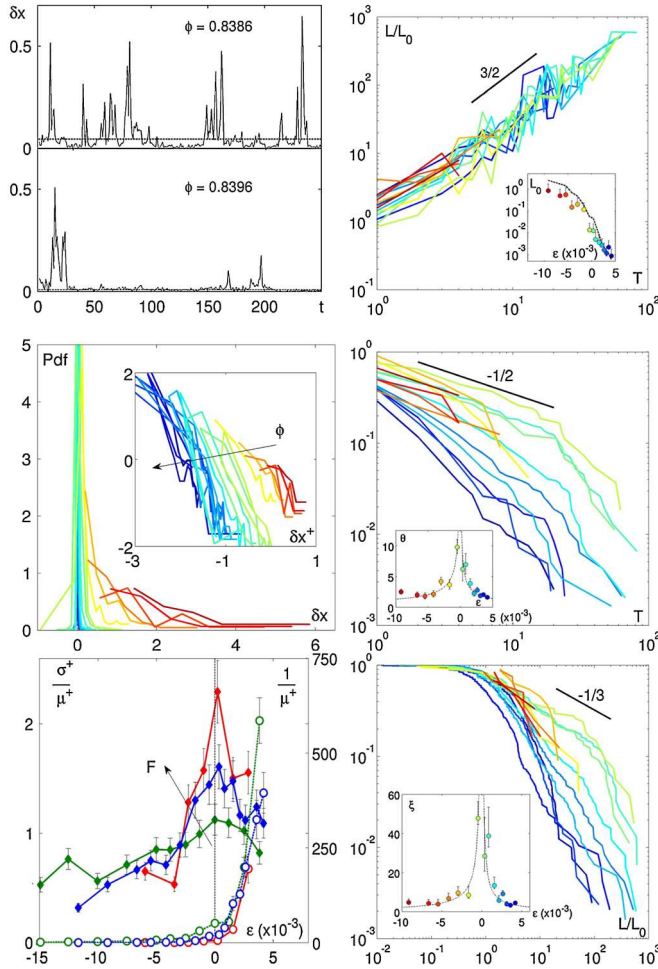


FIG. 3 (color online). Intruder displacements statistics:  $F = F_2$  and packing fractions ranges from  $\phi = 0.8306$  [red (light gray)] to  $0.8418$  [blue (dark gray)] when not otherwise specified. *Top Left*: Instantaneous displacements  $\delta x(t)$  for  $\phi = 0.8386$  and  $\phi = 0.8396$ . *Middle Left*: Distributions of  $\delta x$ . *Inset*: same in log-log. *Bottom Left* Inverse average  $1/\mu^+$  [(○) right axis] and standard deviation over average  $\sigma^+/\mu^+$  [(◆) left axis] of  $\delta x^+$  as a function of the reduced packing fraction  $\epsilon$  for the three applied force  $F_1$  [red (light gray)],  $F_2$  [blue (dark gray)] and  $F_3$  [green (medium gray)]. *Top Right*: Scaling of the rescaled size  $L/L_0$  of the bursts with their duration  $T$ . *Inset*:  $L_0$  and  $V$  (black dotted line) as a function of  $\phi$ . *Middle Right*: Cumulated distributions of the durations  $T$  of the displacement bursts; *Inset*: Cutoff of the distributions  $\theta(\epsilon)$  versus  $\phi$ . *Bottom Right*: Cumulated distributions of the rescaled size  $L/L_0$ . *Inset*: Cutoff of the distributions  $\xi(\epsilon)$  versus  $\phi$ .

distance to  $\phi_J$  for the three dragging forces. The peak in the fluctuations is clearly separated from the divergence of  $1/\mu^+$  and is a new signature of the jamming transition.

To complete the characterization of the intruder motion, we analyze the duration  $T$  and the size  $L$  associated with the displacement bursts, as is commonly done in crackling noise or Barkhausen noise experiments [13]. We impose a given reference level  $\delta x_0$  and define bursts as the period of times where  $\delta x$  is above this level. The duration  $T$  of a given burst is defined as the interval within two successive

intersections of  $\delta x$  with  $\delta x_0$ , while the size  $L$  is defined as the integral of  $\delta x$  between the same points. Figure 3, top right, shows that  $L(\phi, T) \sim L_0(\phi)T^{1/z}$ , with a dynamical exponents  $z = 2/3$ , and  $L_0$  a scaling length, which can be interpreted as a typical value of  $L$ . Note that it is different from its average value because of the power-law shape of the distributions of  $L$ . Indeed, despite some weakness of our statistics, the cumulated distributions of  $T$  (Fig. 3, middle right), respectively of  $L/L_0$  (Fig. 3, bottom right) can be described as power laws truncated by a scaling function:  $T^{-\alpha}f(T/\theta(\phi))$ , respectively  $(L/L_0)^{-\beta}g(L/\xi(\phi))$ . The cutoff dependence on the packing fraction  $\theta(\phi)$ , resp.  $\xi(\phi)$  are estimated by computing the averages of  $T$ , resp.  $L/L_0$  and display a diverging behavior at  $\phi_J$ :  $\theta(\phi) \propto |\phi - \phi_J|^{-\eta}$ , resp.  $\xi(\phi) \propto |\phi - \phi_J|^{-\nu}$ . Our statistics are not large enough to extract precisely the exponents  $\alpha$ ,  $\beta$ ,  $\eta$  and  $\nu$ ; however estimates of  $\alpha = 1/2$ ,  $\beta = 1/3$ ,  $\eta = 2/3$  and  $\nu = 1$  are consistent with the data and satisfy the relations  $\alpha z = \beta$  and  $\eta = \nu z$ . Also, the same analysis performed on the kinetic energy of the surrounding grains—not shown here—is consistent with the above determination. The dynamical exponent  $z = 2/3$ , different from the  $1/2$  value expected for inertial mechanisms, underlines the role played by the collective dissipative mechanisms.

Finally, we characterize the dynamics around the intruder. The averaged displacement field (Fig. 4, top left) is composed of two symmetric recirculation vortices. This pattern is very robust as evidenced by the shape invariance of the displacement profiles along the direction perpendicular to the drag (Fig. 4, top right). In particular, the exponential decay of the displacement amplitude keeps the same characteristic length across the transition (see inset). Such a smooth and continuous behavior is in contrast with the existence of the sharp transition described above and must be related to the similar absence of signature of the transition when considering the average relaxation time or  $\mu^+(\phi)$ . Again the transition is to be found in the strongly heterogeneous instantaneous displacement field (Fig. 1, right), which exhibits characteristic chainlike motions. This tendency of forming chainlike motions is strongly enforced for a packing fraction larger than  $\phi_J$ . We also compute the averaged free volume, extracted from Laguerre's tessellation of the packing, around the intruder (Fig. 4, bottom left) and observe a small asymmetry between the front and the back of the intruder. Computing for instance the average free volume in a small window in front of and behind the intruder (see Fig. 4, bottom right), one sees that below  $\phi_J$  there is a significant excess of free volume leaving like a “wake” far behind the intruder, whereas above  $\phi_J$  this asymmetry rapidly vanishes together with a strong decrease of the available free volume.

Altogether, the following pictures emerge. The jamming transition, which is marked by a critical behavior of the fluctuations of the intruder displacements separate a regime where the intermittent motion is dominated by rapid

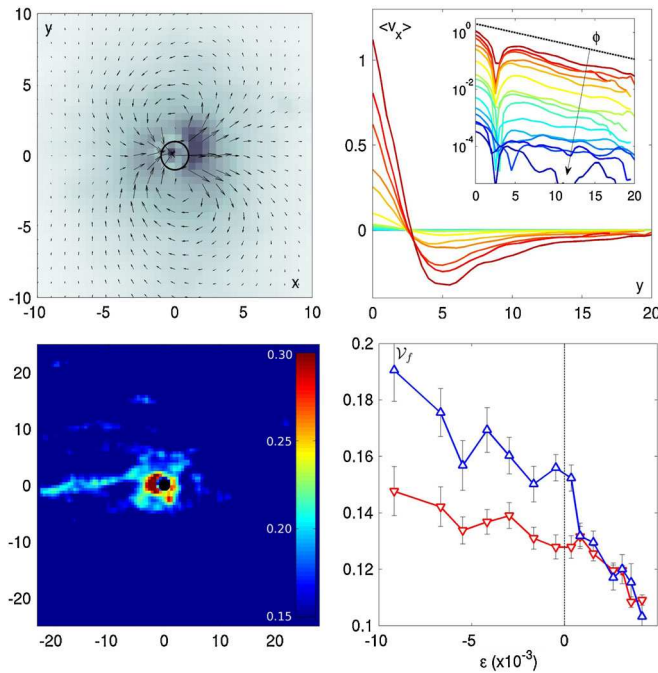


FIG. 4 (color online). Displacements and free volume around the intruder (the intruder goes from left to right;  $F = F_2$ ,  $\phi = \phi_j = 0.8386$ ). *Top Left*: Interpolated average displacement field: the darker, the faster. *Top Right*:  $y$  profiles of the average velocity along the drag direction (same packing fractions as in Fig. 3). *Bottom Left*: Average free volume field. *Bottom Right*: Average free volume vs  $\epsilon$  in front (red  $\nabla$ ) and behind (blue  $\triangle$ ) the intruder.

reorganization of the free volume from one where the motion takes the form of chainlike structures, which are very much reminiscent of the strong force network suggesting the dominant role of the stress fluctuations [16]. Note that the frictional force with the bottom plane is completely negligible as compared to the drag force and the displacements' distribution of the intruder is completely determined by the *collective resistance* of the other grains organized in chain forces. As compared to previous studies of the motion of an intruder in a granular packing [8–11], we have confirmed the transition from a linear viscosuslike dependence of the dragging force with the velocity in the fluidized regime to a logarithmic dependence in the intermittent one. The originality of the present study is to unveil critical features *inside* the intermittent regime and associate them with the jamming transition. The observation of “crackling noise” statistics suggests a possible deeper correspondence in the underlying physical properties with other intermittent phenomena such as the creep motion observed under yield stress in amorphous media [17], the subcritical material failure [18] and more generally, the pinning-depinning transition [19]. We be-

lieve that performing the kind of microrheology experiment sketched out in the present study is a promising path for a better understanding of the jamming of frictional systems.

We would like to thank L. Ponson for having suggested the “crackling noise” analysis, E. Bouchaud, and S. Aumaitre for helpful discussions, as well as F. Paradis, B. Saint-Yves and C. Coulais. We also thank V. Padilla and C. Gasquet for technical assistance on the experiment. This work was supported by ANR DYNHET 07-BLAN-0157-01.

- 
- [1] Jaeger *et al.*, *Rev. Mod. Phys.* **68**, 1259 (1996); A. Liu and S. Nagel, *Nature (London)* **396**, 21 (1998); Cates *et al.*, *Phys. Rev. Lett.* **81**, 1841 (1998); M. Falk and J. Langer, *Phys. Rev. E* **57**, 7192 (1998); Varnik *et al.*, *J. Chem. Phys.* **120**, 2788 (2004); C. Maloney and A. Lemaitre, *Phys. Rev. Lett.* **93**, 195501 (2004); M. Wyart, *Ann. Phys. (Paris)* **30**, 1 (2005).
  - [2] Dollet *et al.*, *Phys. Rev. E* **71**, 031403 (2005).
  - [3] Habdas *et al.*, *Europhys. Lett.* **67**, 477 (2004).
  - [4] N. Xu and C. O’Hern, *Phys. Rev. E* **73**, 061303 (2006); P. Coussot, *Rheometry of Pastes, Suspensions, and Granular Materials* (John Wiley & Sons, New York, 2005); Da Cruz *et al.*, *Phys. Rev. E* **66**, 051305 (2002).
  - [5] G. Marty and O. Dauchot, *Phys. Rev. Lett.* **94**, 015701 (2005); Dauchot *et al.*, *Phys. Rev. Lett.* **95**, 265701 (2005); A. Abate and D. Durian, *Phys. Rev. E* **74**, 031308 (2006); A. Keys *et al.*, *Nature Phys.* **3**, 260 (2007).
  - [6] Lechenault *et al.*, *Europhys. Lett.* **83**, 46 003 (2008).
  - [7] Howell *et al.*, *Phys. Rev. Lett.* **82**, 5241 (1999); G. MiDi, *Eur. Phys. J. E* **14**, 341 (2004); D. Fenistein and M. van Hecke, *Nature (London)* **425**, 256 (2003).
  - [8] Zik *et al.*, *Europhys. Lett.* **17**, 315 (1992); Kolb *et al.*, *Phys. Rev. E* **69**, 031306 (2004).
  - [9] Albert *et al.*, *Phys. Rev. Lett.* **82**, 205 (1999); Chehata *et al.*, *Phys. Fluids* **15**, 1622 (2003).
  - [10] J. Geng and R. Behringer, *Phys. Rev. E* **71**, 011302 (2005).
  - [11] Dalton *et al.*, *Phys. Rev. Lett.* **95**, 138001 (2005); Baldassari *et al.*, *Phys. Rev. Lett.* **96**, 118002 (2006).
  - [12] Hastings *et al.*, *Phys. Rev. Lett.* **90**, 098302 (2003); Leonforte *et al.*, *Phys. Rev. B* **70**, 014203 (2004).
  - [13] C. R. M. James, P. Sethna, and Karin A. Dahmen, *Nature (London)* **410**, 242 (2001); G. Durin and S. Zapperi, in *The Science of Hysteresis*, edited by Bertotti and Mayergoyz (Academic Press, Amsterdam, 2006).
  - [14] G. Parisi and F. Zamponi, arXiv:0802.2180 [*Rev. Mod. Phys.* (to be published)].
  - [15] L. Berthier and T. Witten, *Europhys. Lett.* **86**, 10001 (2009).
  - [16] Howell *et al.*, *Phys. Rev. Lett.* **82**, 5241 (1999).
  - [17] Falk *et al.*, *Phys. Rev. E* **70**, 011507 (2004).
  - [18] Bonamy *et al.*, *Phys. Rev. Lett.* **101**, 045501 (2008).
  - [19] Chauve *et al.*, *Phys. Rev. B* **62**, 6241 (2000).